Supporting Information

High performance Juncus effusus cellulosic adsorbent modified with citric acid and magnetic Fe_3O_4 for dye wastewater

Keming Zhou,[a] Lianpeng Yan,[a] Rui Zhang,[*a,b] and Xuedong Zhu[a]

a. Engineering Research Centre of Large Scale Reactor Engineering and Technology, Ministry of Education, School of Chemical Engineering, East China University of Science and Technology, 130 Meilong Road, Shanghai 200237, China.

b. Shanghai Key Laboratory of Green Chemistry and Chemical Processes, East China Normal University, School of Chemistry and Molecular Engineering, Shanghai 200062, China.

* Corresponding authors.

E-mail address: r.zhang@ecust.edu.cn (R. Zhang).

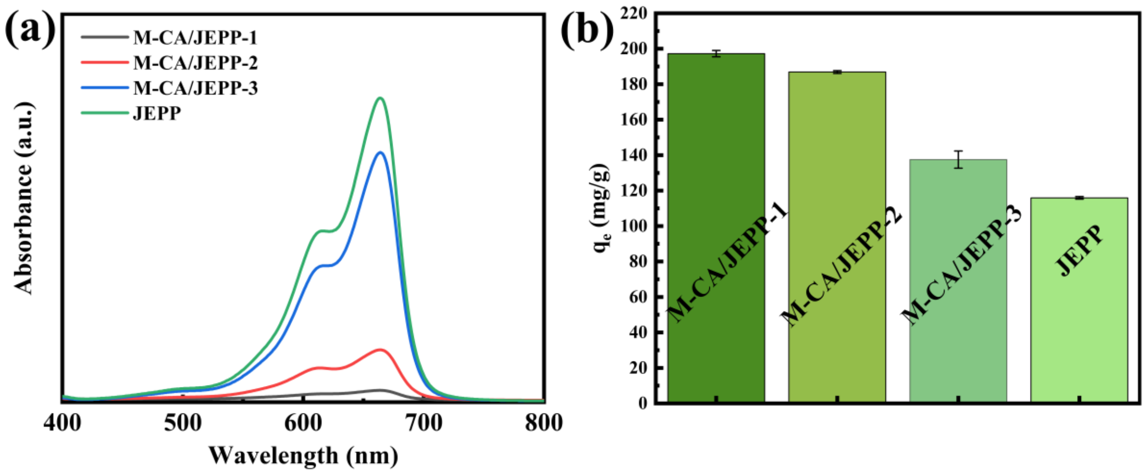

Fig. S1 UV-Vis absorption spectrum a) and the equilibrium adsorption capacity b) using different adsorbents, pH=11, initial dye concentration of 100 mg/L, 303 K and 10 mg of absorbents

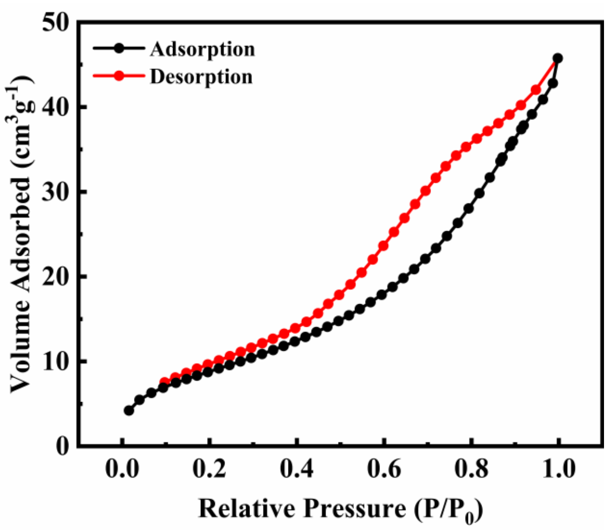

Fig. S2 The nitrogen adsorption-desorption isotherm of M-CA/JEPP

The measurement of nitrogen adsorption-desorption isotherms and the Brunauer–Emmett–Teller (BET) surface area towards M-CA/JEPP was carried out. As seen from **Fig. S2**, the isotherm could be classified as type IV with an apparent hysteresis loop, revealing the presence of mesopores. The BET specific surface area of M-CA/JEPP was 34.15 m^2/g.

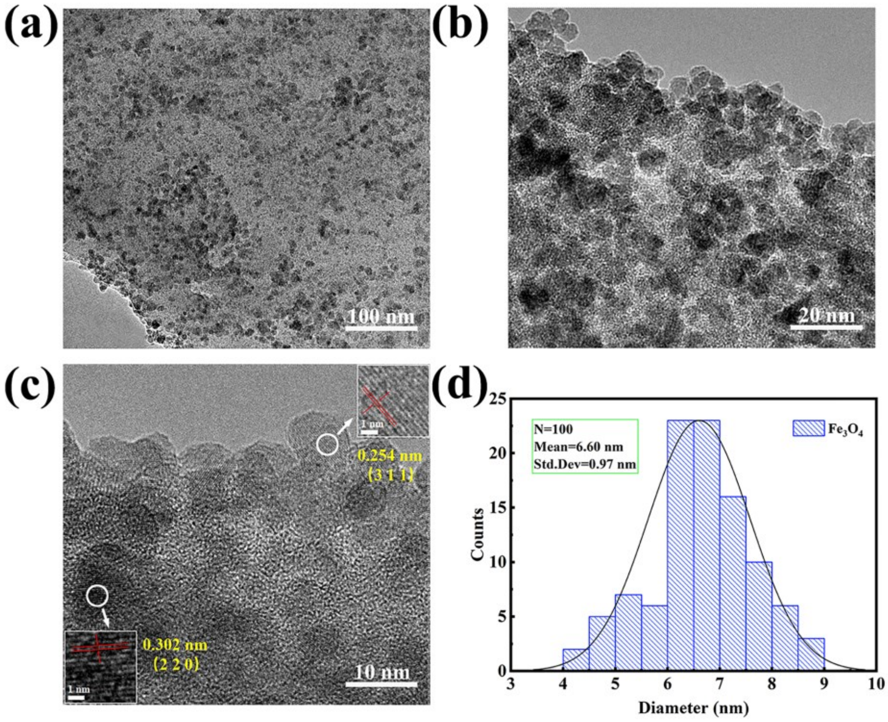

Fig. S3 TEM images of (a-c) M-CA/JEPP; (d) Size distribution histogram of the synthesized Fe_3O_4 nanoparticles

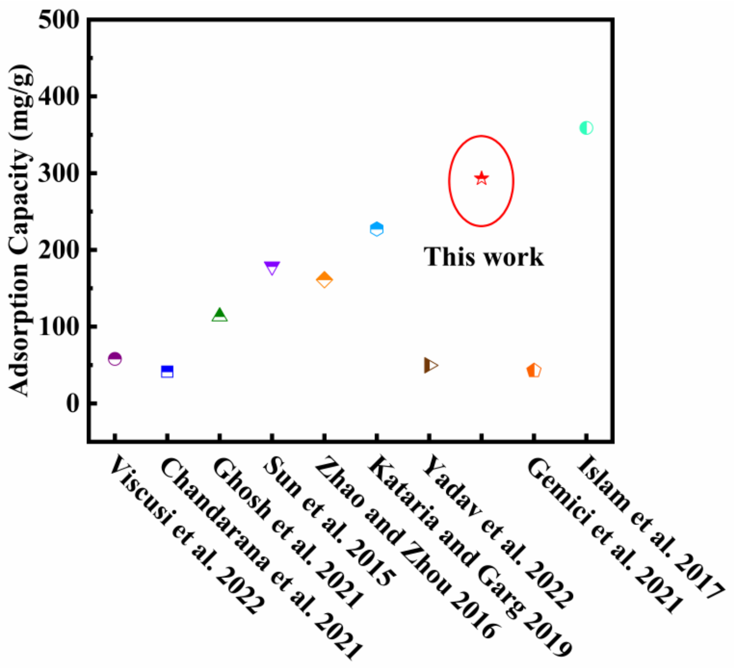

Fig. S4 The M-CA/JEPP for MB compared with other reported adsorbents (Chandarana et al. 2021; Gemici et al. 2021; Ghosh et al. 2021; Islam et al. 2017; Kataria and Garg 2019; Sun et al. 2015; Viscusi et al. 2022; Yadav et al. 2022; Zhao and Zhou 2016)

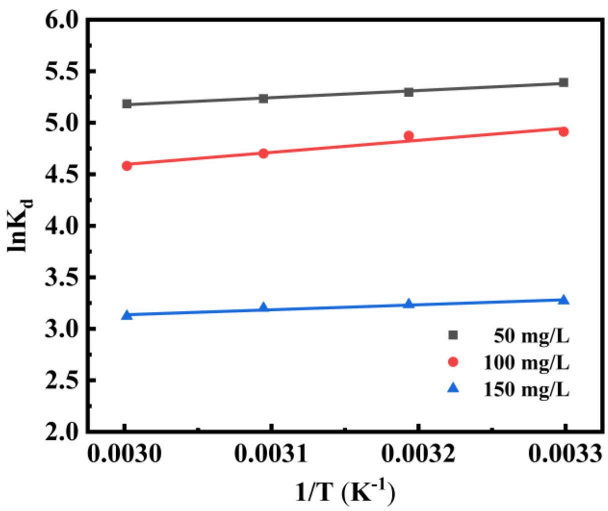

Fig. S5 Thermodynamic fitting of MB adsorption at different concentrations

Adsorption kinetic models:

Pseudo-first-order model:

$$q_t = q_e(1 - e^{-k_1 t}) \tag{S1}$$

Pseudo-second-order model:

$$q_t = \frac{q_e{}^2 k_2 t}{1 + q_e k_2 t} \tag{S2}$$

Intraparticle diffusion model:

$$q_t = \frac{1}{\beta}\ln(\alpha\beta) + \frac{1}{\beta}\ln t \tag{S3}$$

Elovich model:

$$q_t = k_{p,i} t^{\frac{1}{2}} + C_i \tag{S4}$$

where q_t (mg/g) and q_e (mg/g) are the adsorption capacity of dye adsorbed at time t (min) and at equilibrium, respectively. k_1 (min^{-1}) and k_2 (g mg^{-1} min^{-1}) are rate constants for pseudo-first-order and pseudo-second-order models, respectively. α (mg g^{-1} min) and β (g/mg) are the initial adsorption rate and the desorption coefficient for Elovich model, respectively. $k_{p,i}$ (mg g^{-1} min$^{-0.5}$) and C_i (mg/g) are the rate constant of the intraparticle diffusion model and the constant related to the thickness of the boundary layer, respectively.

Adsorption isotherm models:

Langmuir model:

$$q_e = \frac{q_{max} k_l C_e}{1 + k_l C_e} \tag{S5}$$

Freundlich model:

$$q_e = k_f C_e{}^{1/n} \tag{S6}$$

Temkin model:

$$q_e = \frac{RT}{b_T}\ln A_T + \frac{RT}{b_T}\ln C_e, \frac{RT}{b_T} = B \tag{S7}$$

where q_{max} (mg/g) and q_e (mg/g) are the maximum adsorption capacity and equilibrium adsorption capacity, respectively. C_e (mg/L) is the equilibrium concentration of dye solution; k_l (L/mg) and k_f [(mg/g)/(mg/L)$^{1/n}$] are empirical constants for Langmuir and Freundlich isotherms; b_T, A_T (L/g) and B (J/mol) are empirical constants for Temkin isotherm. R is gas constant (8.314 J mol^{-1} K^{-1}) and T is temperature (K).

Separation factor:

$$R_L = \frac{1}{1+k_l C_0} \tag{S8}$$

where R_L is a dimensionless separation factor; C_0 (mg/L) is the initial dye concentration; k_l (L /mg) is empirical constants for Langmuir isotherm. The value of R_L predicts whether an adsorption system is irreversible (R_L=0), favorable ($0<R_L<1$), linear (R_L=1), or unfavorable ($R_L>1$).

Adsorption thermodynamic parameters were calculated as follows

$$\ln K_d = \frac{\Delta S}{R} - \frac{\Delta H}{RT} \tag{S9}$$

$$K_d = \frac{q_e}{C_e} \tag{S10}$$

$$\Delta G = \Delta H - T\Delta S \tag{S11}$$

where K_d is the distribution coefficient; C_e (mg/L) and q_e (mg/g) are the equilibrium concentration and adsorption capacity of dye solution, respectively. ΔG (kJ/mol), ΔS (kJ mol^{-1} K^{-1}) and ΔH (kJ/mol) are Gibbs free energy change, entropy change and enthalpy change, respectively. R is gas constant (8.314 J mol^{-1} K^{-1}) and T is temperature (K).

Table S1 M-CA/JEPP adsorbent samples made under various conditions

Samples	JEPP (g)	$FeCl_3 \cdot 6H_2O$ (g)	$FeSO_4 \cdot 7H_2O$(g)
JEPP	0.926	0	0
M:CA/JEPP-1	0.926	1.081	0.695
M:CA/JEPP-2	0.926	2.162	1.390
M:CA/JEPP-3	0.926	4.324	2.780

Table S2 Thermodynamic parameters for different initial concentrations of MB on M-CA/JEPP

Initial concentration (mg/L)	Temperature (K)	Thermodynamic parameters		
		ΔH (kJ/mol)	*ΔS* [kJ/(mol K)]	*ΔG* (kJ/mol)
50	303	-5.755	0.026	-13.558
50	313			-13.816
50	323			-14.073
50	333			-14.331
100	303	-9.752	0.009	-12.463
100	313			-12.553
100	323			-12.642
100	333			-12.731
150	303	-4.039	0.014	-8.268
150	313			-8.407
150	323			-8.547
150	333			-8.686

Reference

Chandarana H, Senthil Kumar P, Seenuvasan M, Anil Kumar M (2021) Kinetics, equilibrium and thermodynamic investigations of methylene blue dye removal using Casuarina equisetifolia pines. Chemosphere 285:131480. https://doi.org/10.1016/j.chemosphere.2021.131480

Gemici BT, Ozel HU, Ozel HB (2021) Removal of methylene blue onto forest wastes: Adsorption isotherms, kinetics and thermodynamic analysis. Environ Technol Inno 22:101501. https://doi.org/10.1016/j.eti.2021.101501

Ghosh I, Kar S, Chatterjee T, Bar N, Das SK (2021) Removal of methylene blue from aqueous solution using Lathyrus sativus husk: Adsorption study, MPR and ANN modelling. Process Saf Environ Prot 149:345-361. https://doi.org/10.1016/j.psep.2020.11.003

Islam MA, Ahmed MJ, Khanday WA, Asif M, Hameed BH (2017) Mesoporous activated carbon prepared from NaOH activation of rattan (Lacosperma secundiflorum) hydrochar for methylene blue removal. Ecotoxicol Environ Saf 138:279-285. https://doi.org/10.1016/j.ecoenv.2017.01.010

Kataria N, Garg VK (2019) Application of EDTA modified Fe_3O_4/sawdust carbon nanocomposites to ameliorate methylene blue and brilliant green dye laden water. Environ Res 172:43-54. https://doi.org/10.1016/j.envres.2019.02.002

Sun L, Chen DM, Wan SG, Yu ZB (2015) Performance, kinetics, and equilibrium of methylene blue adsorption on biochar derived from eucalyptus saw dust modified with citric, tartaric, and acetic acids. Bioresour Technol 198:300-308. https://doi.org/10.1016/j.biortech.2015.09.026

Viscusi G, Lamberti E, Gorrasi G (2022) Hemp fibers modified with graphite oxide as green and efficient solution for water remediation: Application to methylene blue. Chemosphere 288:132614. https://doi.org/10.1016/j.chemosphere.2021.132614

Yadav SK, Dhakate SR, Pratap Singh B (2022) Carbon nanotube incorporated eucalyptus derived activated carbon-based novel adsorbent for efficient removal of methylene blue and eosin yellow dyes. Bioresour Technol 344:126231. https://doi.org/10.1016/j.biortech.2021.126231

Zhao SX, Zhou TS (2016) Biosorption of methylene blue from wastewater by an extraction residue of Salvia miltiorrhiza Bge. Bioresour Technol 219:330-337. https://doi.org/10.1016/j.biortech.2016.07.121